Conducting tip atomic force microscopy analysis of aluminum oxide barrier defects decorated by electrodeposition

J. Carrey, K. Bouzehouane, J.-M. George, C. Ceneray, A. Fert et al.

Citation: Appl. Phys. Lett. **79**, 3158 (2001); doi: 10.1063/1.1415775
View online: http://dx.doi.org/10.1063/1.1415775
View Table of Contents: http://apl.aip.org/resource/1/APPLAB/v79/i19
Published by the American Institute of Physics.

Conducting tip atomic force microscopy analysis of aluminum oxide barrier defects decorated by electrodeposition

J. Carrey,[a] K. Bouzehouane, J.-M. George, C. Ceneray, A. Fert, and A. Vaurès
Unité Mixte de Physique CNRS/THALES, Domaine de Corbeville, 91404 Orsay Cedex, France and Université Paris-Sud, 91405 Orsay Cedex, France

S. Kenane and L. Piraux
Unité de Physico-Chimie et de Physique des Matériaux, Université Louvain-La-Neuve, Place Croix du Sud, 1348 Louvain-La-Neuve, Belgium

(Received 11 June 2001; accepted for publication 27 August 2001)

We show that the electrodeposition of $Ni_{80}Fe_{20}$ on top of a thin aluminum oxide barrier leads to particle growth occurring on preferential nucleation centers. The particle sites are attributed to local defects in the aluminum oxide barrier. As a function of the thickness of the barrier, different growth modes can occur. For thinner barriers, new nucleation centers are created during electrodeposition. The resistance of the defects, characterized by conducting atomic force microscopy, ranges from less than 10^4 to greater than $10^{12}\,\Omega$. Various $I(V)$ characteristics were also obtained, depending on the resistance of the defect. These results suggest that this experimental technique could be a very interesting one with which to fabricate nanoconstrictions dedicated to ballistic magnetoresistance studies. © *2001 American Institute of Physics.* [DOI: [10.1063/1.1415775]

In research on magnetic tunnel junctions,[1] ''pinholes'' are generally viewed as defects which spoil the properties of the junctions. These pinholes, associated with direct metallic contacts or due to stoichiometric defects, give rise to additional conduction channels through the junction barrier. On the other hand, pinholes can be useful defects if they are filled by electrodeposition to fabricate nanocontacts between two metals and to investigate magnetotransport properties of nanocontacts. In particular, this fabrication method can be of interest to study ballistic magnetoresistance (BMR) which has recently been found in nanocontacts between two ferromagnetic metals.[2–4]

Until now, these nanocontacts have been fabricated one by one by mechanical or chemical methods which complicate the study of magnetic and transport properties. Of the different pinholes in a thin insulating barrier, some of them should present the right conditions to observe BMR. With the interest in ballistic transport mechanisms, this experimental approach should be useful to electrically characterize the different types of defects and the role they may play in tunnel junction devices.

Up to now, two different methods have been used to image pinholes in tunnel junctions: direct measurement of the local tunnel current using conducting tip atomic force microscopy (AFM)[5–7] and defect decoration by electrodeposited metal.[8] The first method allows one to measure variations of the local conductivity by scanning a surface. However it cannot be used to establish stable contact of the pinhole because the AFM cannot be permanently maintained at the same position. Moreover, the size of the tip does not allow the measurement of small topographic defects. The second method seems very promising but a lot of questions remain. Are the defects created by the electrodeposition method? What is the resistance and the nature of such defects? What is the relation, if any, between the size of the electrodeposited particles and the resistance of the defects?

In this letter, we present results which lead to significant progress in the understanding of particle growth mechanisms and in defect characterization by combining the electrodeposition of a ferromagnetic material such as $Ni_{80}Fe_{20}$ (permalloy) on various thickness tunnel barriers with current mapping using a conducting tip AFM.

Samples were grown in an Alcatel 610 sputtering apparatus and have the following structure: $Al_2O_3/Ni_{80}Fe_{20}$-150 Å/Si. The Al_2O_3 barrier was fabricated by oxidation of Al in an Ar/O_2 plasma. The partial pressure of both gazes are 2 mTorr. Samples with Al thicknesses of 10, 15, 20 and 25 Å were studied. The oxidation times were previously optimized during study of tunnel junctions[9] to fully oxidize the Al layer but not the NiFe layer. Two criteria were used: the small temperature dependence of the resistance and the maximization of the tunnel magnetoresistance effect. From transmission electron microscopy (TEM) experiments, the aluminum oxide barriers were found to be amorphous, with a thickness 1.5 larger than the deposited Al in agreement with the expected value for crystalline alumina (Al_2O_3). The conducting tip AFM we used is the same as that fabricated by Houzé *et al.*[10] and has a resistance measurement range from 100 to $10^{12}\,\Omega$ with bias voltage ranging from 0.1 to 10 V. Prior to electrodeposition, we observed samples with different barrier thicknesses: no current contrast was found on any of the samples with a bias of 1 V, implying that the local resistance always exceeded $10^{12}\,\Omega$.

To perform electrodeposition, we used a bath of Ni sulfate and Fe sulfate with concentrations of 0.5 and 0.02 M, respectively. A concentration of 0.4 M of boric acid was added as a chemical buffer to limit a *p*H rise at the surface. The electrolyte temperature was maintained at 25 °C. No chemical additives were used because these species are often incorporated into the deposit. The deposition was controlled

[a]Electronic mail: julian.carrey@thalesgroup.com

by an EG&G model 263 potentiostat/galvanostat. The permalloy was deposited at -1 V relative to Ag/AgCl electrode. A pure Ni plate was used as a counterelectrode. The composition of the deposited particles was determined by a ICP-AES1 spectrophotometer.

The first observation of the permalloy particles was performed with scanning electron microscopy (SEM). The density of the particles for barriers with 10, 15, 20 and 25 Å of Al were, respectively, about 50 000, 6000, 150 and 75 mm^{-2}.

The electrodeposition current provides precious information about the growth mechanisms of such structures. One must first distinguish between samples with thick barriers (20 and 25 Å Al) and thinner ones (10 and 15 Å). Thicker samples exhibit regular electrodeposition curves, characteristic of a fixed density of particles all growing at the same rate on a given density of pinholes, as we will see below. SEM observations on such samples show that particles indeed have a very narrow size distribution. In thinner samples, the current shows sudden increases, the electrodeposition curves are nonreproducible from sample to sample, and a large distribution in particle size is seen by SEM. It seems clear that, in this case, new nucleation centers are created during the electrodeposition process itself. For thicker samples, pinholes are not created during electrodeposition but we cannot exclude that they could be created by the applied voltage necessary to begin electrodeposition.[11]

When a particle grows on a defect, the electrodeposition current can be limited by the resistance of the defect and/or by the charge transfer in the solution. At low coverage, each particle can be considered independent of its neighbors. Under these conditions, if the resistance of the defect does not limit growth, one expects (a) the current to be proportional to the substrate surface covered by particles and (b) that if the particle density is constant during growth, the current must increase with the surface of the particles, and so with the square of time.[12] Condition (a) is indeed verified for all samples with low particle coverage ($<5\%$) and (b) is verified for all samples with high barrier thicknesses [see Figs. 1(a) and 1(b)]. Knowing the surface of the electrodeposition cell, one can extract[13] from Fig. 1(a) a surface resistance R_S due to the reaction. Using the density of particles extracted from SEM observations, R_S can also be derived[13] from Fig. 1(b). Both curves are in good agreement and give $R_S = 38 \pm 5\ \Omega\mathrm{cm}^2$. This value means that, if we consider a defect with a resistance of, for example, 3 MΩ in series with the particle, the resistance will start to limit the electrodeposition current when the particle has reached a diameter of 1 μm. These observations confirm that no new defects are created during electrodeposition on thicker barriers. For a higher coverage of particles on the substrate, conditions (a) and (b) are no longer verified as the current progressively saturates. This saturation is due to limitation in the maximum current capable of circulating in the solution and to the resistance of the defects. When performing electrodeposition onto a metallic substrate, the current is indeed limited to 600 μA.

The samples were observed after electrodeposition with a conducting tip AFM. As the thickness of the barrier increases, it becomes more and more difficult, on the AFM scale, to localize the particles and consequently to perform statistical studies. This is why we only report on the sample,

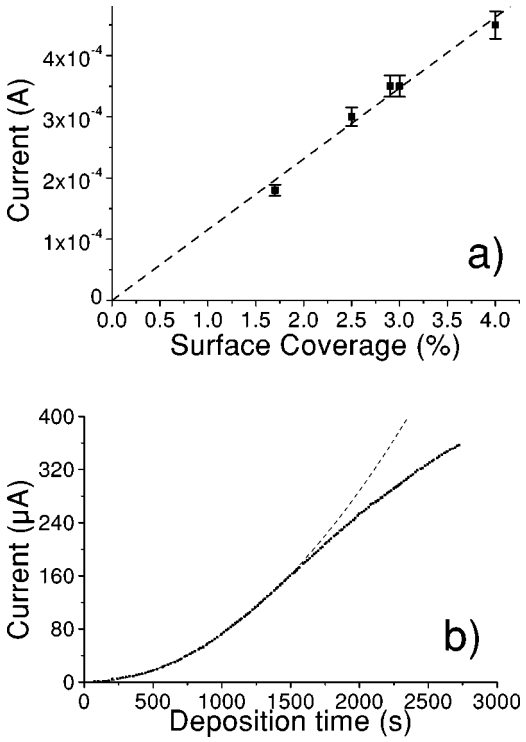

FIG. 1. (a) Current at the end of the electrodeposition process as a function of the particle surface coverage for samples with various barrier thicknesses (from 10 to 25 Å of Al) and low particle coverage. (b) Electrodeposition current i as a function of time t for a sample with 25 Å of Al. The initial part of the curve is fit by the function $i \sim t^2$. Similar curves are seen for samples with barriers of 20 and 25 Å of Al.

with the thinnest barrier. Figure 2 shows an example of a conducting tip AFM scan with topographic (right side) and resistance (left side) maps of the same area of the sample. Aside from the particles, on the alumina background the measured local resistance of the barrier is above $10^{12}\,\Omega$, as measured prior to electrodeposition. In contrast, several particles have resistances around $6 \pm 2 \times 10^3\,\Omega$, which is the resistance of the AFM conducting tip. We conclude that the resistance of these particles is therefore lower. Particles 1–5 have resistances at 1 V of, respectively, 1.1×10^4, 2.1

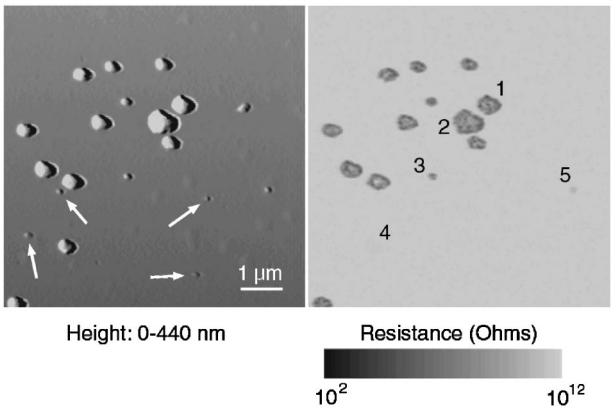

FIG. 2. Example of images acquired with the conducting tip AFM for a sample with 10 Å of Al, electrodeposited for 600 s. The image on the left is topographical and that on the right is a current image, with a bias of 1 V. Particles 1–5 have resistances at 1 V of, respectively. 1.1×10^4, 2.1×10^4, 3.5×10^4, 1.1×10^{10}, and $1.1 \times 10^{11}\ \Omega$. Four small size particles have resistance above $10^{12}\ \Omega$ so they are seen in the topographic image but not in the resistance one (white arrows).

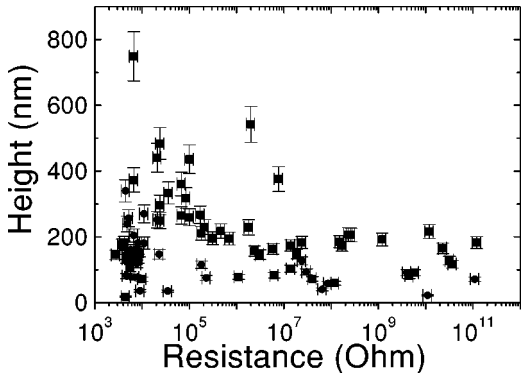

FIG. 3. Particle height vs its corresponding electrical resistance as measured by the AFM, for the sample with 10 Å of Al electrodeposited for 600 s. The bias voltage applied during the conducting tip the AFM analysis was 1 V.

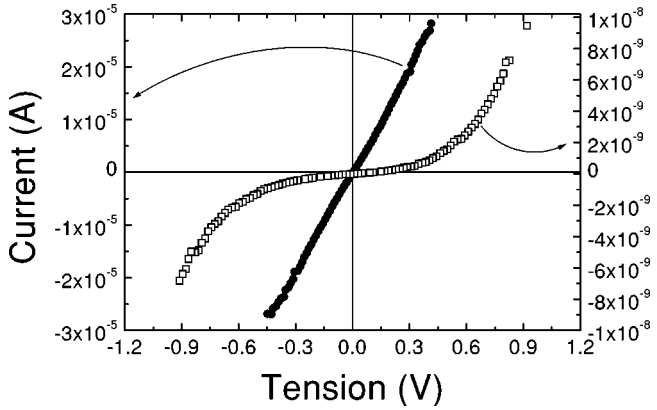

FIG. 4. $I(V)$ of two different particles of the sample with 10 Å of Al, electrodeposited for 600 s.

$\times 10^4$, 3.5×10^4, 1.1×10^{10}, and $1.1\times 10^{11}\,\Omega$. There are also four small size particles which have resistance above $10^{12}\,\Omega$ so they are seen in the topographic image but not in the resistance one (see white arrows). In Fig. 3, we plot the particle height against its electrical resistance as measured by the AFM and for particles found on different areas of the sample. As was discussed above, the very high resistance of some defects limits the size of the particle which grows on it. This explains why no particle higher than 200 nm can be found for defects whose resistance is higher than $10^{10}\,\Omega$. On the other hand, one can find small particles with small resistances. These particles have nucleated later in the deposition, as we already mentioned when we used thin barrier samples, so they did not have time to reach a great height. These defects also show differences in their $I(V)$ characteristics. Low resistance defects have ohmic resistance while high resistance ones have nonlinear characteristics. Two representative examples of these $I(V)$ curves are presented in Fig. 4.

In summary, we have shown that, when electrodeposing permalloy on an amorphous alumina tunnel barrier, two different growth modes can occur, depending on the barrier thickness. For thin barriers, new particles nucleate during electrodeposition. By using a conducting tip AFM, we have shown that the defects revealed by this method have a very large distribution in resistance, ranging from less than 10^4 to greater than $10^{12}\,\Omega$, and present various associated $I(V)$ characteristics. These results suggest that this experimental approach could be a very interesting one by which to fabricate nanoconstrictions dedicated to BMR study.

The authors thank F. Houzé and O. Schneegans of Laboratoire de Génie Electrique de Paris for providing the apparatus and for stimulating discussions, and M. Bowen for his careful reading of the manuscript. One of the authors (L.P.) is a research associate for the National Fund for Scientific Research (Belgium). This work was partly supported by the Belgian Interuniversity Attraction Pole Program (PAI-IUAP P4/10).

[1] J. S. Moodera, L. R. Kinder, T. M. Wong, and R. Meservey, Phys. Rev. Lett. **74**, 3273 (1995).
[2] N. Garcia, M. Munoz, and Y.-W. Zhao, Phys. Rev. Lett. **82**, 2923 (1999).
[3] G. Tatara, Y.-W. Zhao, M. Munoz, and N. Garcia, Phys. Rev. Lett. **83**, 2030 (1999).
[4] N. Garcia, H. Rohrer, I. G. Saveliev, and Y.-W. Zhao, Phys. Rev. Lett. **85**, 3053 (2000).
[5] V. D. Costa, C. Tiusan, T. Dimopoulos, and K. Ounadjela, Phys. Rev. Lett. **85**, 876 (2000).
[6] Y. Ando, H. Kameda, H. Kubota, and T. Miyazaki, J. Appl. Phys. **87**, 5206 (2000).
[7] Y. Ando, H. Kameda, H. Kubota, and T. Miyazaki, J. Appl. Phys. **38**, L737 (1999).
[8] R. Schad, D. Allen, G. Zangari, I. Zana, D. Yang, M. Tondra, and D. Wang, Appl. Phys. Lett. **76**, 601 (2000).
[9] J. Nassar, M. Hehn, A. Vaures, F. Petroff, and A. Fert, Appl. Phys. Lett. **73**, 698 (1998).
[10] F. Houzé, R. Meyer, O. Schneegans, and L. Boyer, Appl. Phys. Lett. **69**, 1975 (1996).
[11] D. Allen, R. Shad, G. Zangari, I. Zana, D. Yang, M. Tondra, and D. Wang, J. Vac. Sci. Technol. A **18**, 1830 (2000).
[12] The volume V of the particle verifies $V(t)\sim\int i(t)$. If we suppose that $i(t)\sim S(t)$, where S is the surface of the particle, one can easily deduce that $i(t)\sim t^2$.
[13] R_S can be derived from Fig. 1(a) in the following way: we extract from the data the relation $i=A\Theta$, where i is the current and Θ the coverage. If we assume that particles are hemispherical, R_S can be calculated with the formula $R_S=2U\pi R^2/A$, where U is the electrodeposition bias (1 V) and R the electrodeposition cell radius (2.5 mm). R_S can be derived from Fig. 1(b) in the following way: we extract from the data the relation $i(t)=Bt^2$. Integrating this relation and knowing the number of particles allows one to calculate the size evolution of one particle over time. R_S is then derived simply from these two relations so one finds that $R_S=U((V/ne))^{2/3}((2\pi N/B))^{1/3}$, where V is the atomic volume of the permalloy, n the number of electrons needed to produce one atom (2), e the charge of the electron and N the number of particles.